INFRARED SPECTROSCOPY AND INTEGRATED MOLAR ABSORPTIVITY OF C_{60} AND C_{70} FULLERENES AT EXTREME TEMPERATURES

Susana Iglesias-Groth[1], Franco Cataldo[2,3], Arturo Manchado[1, 4, 5]

[1]Instituto de Astrofísica de Canarias, Via Lactea s/n, E-38200, La Laguna, Tenerife, Spain

[2]Istituto Nazionale di Astrofisica – Osservatorio Astrofisico di Catania, Via S. Sofia 78, 95123 Catania, Italy

[3]Actinium Chemical Research, Via Casilina 1626/A, 00133 Rome, Italy

[4] Consejo Superior de Investigaciones Científicas, Spain

[5] Departamento de Astrofísica, Universidad de La Laguna, E-38205 La Laguna, Tenerife, Spain

Abstract

The detection of C_{60} and C_{70} fullerenes in young planetary nebulae (Cami et al. 2010; Garcia-Hernandez et al. 2010) and in reflection nebulae (Sellgren et al. 2010) suggest that these molecules are more common in certain astrophysical environments than thought before. The dependence on temperature of the positions and widths of the infrared bands of the C_{60} and C_{70} fullerenes is needed for a firm qualitative detection of these molecules in space. Furthermore, the integrated molar absorptivity Ψ (in Km/mol) of each infrared absorption band is required for a quantitative determination of the abundance of C_{60} and C_{70} in space. The present work reports on the temperature dependence of the wavelength shift and integrated molar absorptivity of the infrared bands of C_{60} and C_{70} fullerenes. The measurements were made in a KBr matrix in a wide range of temperatures comprised between -180°C and +250°C. The experimental data were extrapolated to absolute zero for both the infrared band shift and the integrated molar absorptivity of C_{60} and C_{70} fullerenes.

Key words: astrochemistry – fullerenes – methods: laboratory spectroscopy

1. Introduction

The infrared measurements from Spitzer space telescope have led to the detection of the C_{60} fullerene and hints about the possible presence of the larger homologous C_{70} in a young planetary nebula Tc 1 (Cami et al. 2010). The detection of fullerenes in such object comes as a surprise since it is known that the formation of fullerenes require environments completely free from hydrogen (Ehrenfreund and Foing, 2010). Thus, the fullerenes were thought to be formed in the inner core region of Tc 1 which is supposed to be carbon-rich, hydrogen-poor and dusty (Cami et al. 2010). On the other hand, Garcia-Hernandez et al. (2010) have also found with the Spitzer space telescope the presence of C_{60} in the circumstellar medium of a series of different planetary nebulae including

SMP SMC 16, an extragalactic source. Astonishingly C_{60} and C_{70} were found in a hydrogen-rich environment mixed with polycyclic aromatic hydrocarbons (PAHs). As a likely explanation for the simultaneous presence of fullerenes and PAHs, Garcia-Hernandez et al. (2010) have proposed that fullerenes may be formed by the photochemical processing of hydrogenated amorphous carbon (HAC). Experimental studies on the hydrogenation of fullerenes have shown that the infrared spectrum of hydrogenated fullerenes (called fulleranes) is similar to the infrared spectra recorded in certain protoplanetary nebulae (Cataldo, 2003). Fullerenes must necessarily be formed in a hydrogen depleted environment but once formed and exposed to hydrogen undergo easily the hydrogenation to fulleranes (Cataldo and Iglesias-Groth, 2010). UV radiation of fulleranes causes the release of hydrogen and the formation of aromatic derivatives from fullerenes, while the thermal processing of fulleranes produces back the fullerenes (Cataldo and Iglesias-Groth 2009, 2010).
Fullerene C_{60} has also been detected in the interstellar medium and more precisely in the reflection nebulae NGC 7023 and NGC 2023 (Sellgren et al. 2009 and 2010). Once formed, the fullerenes are stable toward high energy radiation and cosmic rays (Cataldo, Strazzulla and Iglesias-Groth, 2009). C_{60} and C_{70} fullerenes are the largest molecules detected in space exceeding in number of atoms the cyanopolyyne H-C_{11}N (Bell et al. 1997) confirmed more than a decade ago, and the very recent tentative detection of anthracene $C_{14}H_{10}$ (Iglesias-Groth et al. 2010). The C_{60} fullerene detection in space represents the culmination of a long standing prediction about their existence formulated by Kroto (1988 and 1992) and Hare and Kroto (1992) about 20 years ago.

The search for fullerenes was concentrated in the circumstellar environment of late-type carbon-rich stars where probably C_{60} is embedded or mixed with other forms of elemental carbon. Particularly remarkable places to search for fullerenes were the *R Coronae Borealis* class of stars (Goeres and Sedlmayr, 1993). These stars are helium-rich carbon giants and present a circumstellar environment particularly favorable for fullerenes formation. However fullerenes were not detected till now in these type of stars (Clayton et al. 1995; Nuccitelli et al. 2005). Fullerenes were expected to be present in space based on theoretical calculations reproducing astrophysical phenomena (Iglesias-Groth 2004, 2006 and 2007) and on their considerable stability toward high energy photons and also toward cosmic rays (Cataldo, Strazzulla and Iglesias-Groth, 2009). When embedded in an amorphous or graphitic matrix C_{60} is expected to be in a neutral state, while if exposed to the space conditions the ionization of C_{60} to C_{60}^{+} is expected due to the relatively low ionization potential. Indeed hints about the presence of C_{60}^{+} in the diffuse interstellar bands were reported by Foing and Ehrenfreund (1994).
From the astrochemistry point of view, it is extremely important to know the low temperature infrared spectra of molecules which are subject of research in space. The vibrational spectroscopy of C_{60} and C_{70} fullerenes has been investigated in numerous papers and reviewed by Kuzmany et al. 1995 and 2000. Much less attention has been dedicated to the low and high temperature spectra of these two molecules (Frum et al. 1991; Nemes et al. 1994; Cataldo, Iglesias-Groth and Manchado, 2010; Cataldo and Iglesias-Groth 2010) and there are no reports at all specifically dedicated to the molar extinction coefficient and the integrated molar absorptivity of C_{60} and C_{70}.
The present work is dedicated to review the low and high temperature infrared spectroscopy of C_{60} and C_{70} fullerenes and to the measurement and disclosure of the molar extinction coefficient and the integrated molar absorptivity of C_{60} and C_{70}.

2. Experimental

2.1 Materials and Equipment

Fullerenes C_{60} and C_{70} were high purity grades (99,95% and 99,0+% respectively) from MTR Ltd, (USA). Potassium bromide (infrared spectroscopy grade) was obtained from Sigma-Aldrich. The

infrared spectra were recorded on a Thermo-Fischer FT-IR spectrometer model Nicolet IR-300 at a resolution of 1 cm^{-1}. The KBr pellet used in the infrared spectra measurement were produced in a Silfradent press equipped with a pressure meter; the KBr pellets were produced at a pressure comprised between 3.0 and 3.5 tonns/cm^2. The thickness of the KBr pellets was measured with a Somet digital micrometer having a sensitivity of 0.01 mm.
The low temperature apparatus consisted of a variable temperature cell from Specac model P/N 21525 equipped with KBr windows and sample holder which is able to work in the range comprised between +250°C to -196°C. The variable temperature cell was evacuated with a Buchi vacuum pump model V-710 equipped with four diaphragm heads and a three-stage vacuum creation process which delivers 3.1 m^3/h and an absolute vacuum of 2 mbar.

2.2 – Measurement of the infrared spectrum and the molar absorptivity and integrated molar absorptivity of C_{60} from low to high temperatures.

C_{60} (2.2 mg) was quickly mixed with 245.4 mg of KBr in a agate mortar and the two components were finely ground together. The powder was transferred into a macro-micro KBr pellet die and compressed at 3.3 tonns/cm^2 with the Silfradent press. The resulting pellet having a measured thickness of 0.71 mm was mounted into the sample holder of the Specac variable temperature cell and inserted into the cell. The cell was then evacuated with the aid of the Buchi pump to a vacuum of 0.1 torr and then heated gradually at +60°C in order to permit the humidity eventually absorbed on the internal surfaces of the cell and in the KBr pellet to evaporate. In order to go below room temperature, use was made of liquid nitrogen, added cautiously and in small amount in the cavity present inside the Specac cell. Such cavity is connected with the sample holder and permits to cool the sample to the desired temperature. The temperature of the sample was monitored with thermocouples present in the cell. The lowest temperature reached with this apparatus was -180°C while the highest temperature was +250°C. Heating is provided by the Joule effect supplied to the Specac cell by an external thermal control unit. A more detailed description of the apparatus (photos) used for the measurement can be found in the book of Cataldo and Iglesias-Groth (2010).
The spectra were recorded in absorbance mode. The measurement of the intensity (height) of the absorption bands with automatic subtraction of the baseline was made through the Ominc software from Thermo, dedicated to the FTIR spectrometer. Similarly, the integrated band intensity was also measured through the Omnic software. Of course, no reaction was observed in the prolonged heating at +250°C of the KBr pellet with C_{60} in the evacuated cell. In fact, the infrared spectrum was not altered by new absorption bands which may imply degradation or reaction of C_{60} with the KBr matrix and on cooling down to room temperature the spectrum was identical to that recorded before heating.

2.3 - Measurement of the infrared spectrum and the molar absorptivity and integrated molar absorptivity of C_{70} from low to high temperatures.

C_{70} (2.3 mg) was quickly mixed with 247.5 mg of KBr in a agate mortar and the two components were finely ground together. The powder was transferred into a macro-micro KBr pellet die and compressed at 3.1 tonns/cm^2 with the Silfradent press. The resulting pellet having a measured thickness of 0.75 mm was transferred in the FTIR spectrometer and the spectra were recorded in absorbance mode under the same conditions just described in the previous section for C_{60}. Also in this case, no reaction was observed after prolonged heating of C_{70} with the KBr matrix at +250°C under vacuum. The infrared spectrum was not altered by new absorption bands which may imply degradation or reaction of C_{70} with the KBr matrix and on cooling down to room temperature the spectrum was identical to that recorded before heating.

3. Results and discussion

3.1 The low temperature and high temperature gas phase FT-IR spectra of C_{60} fullerene

Fullerene C_{60} has the highest symmetry of any known molecule. Although there are 174 vibrational degrees of freedom (3N-6) for each C_{60} molecule, the icosahedral symmetry of the fullerene C_{60} gives rise to a number of degenerate modes, so that only 46 frequency modes are expected for this molecule. Of these, four are infrared-active and 10 are Raman-active, whereas the remaining modes are optically inactive (Kuzmany et al. 1995, 2000). Thus, the infrared spectrum of C_{60} is very simple consisting of four modes with F_{1u} symmetry observed at frequencies of 527 ($F_{1u}(1)$), 576 ($F_{1u}(2)$), 1182 ($F_{1u}(3)$) and 1429 ($F_{1u}(4)$) cm^{-1}. The 527 and 576 cm^{-1} modes are associated with a primarily radial motion of the carbon atoms, while the 1182 and 1427 cm^{-1} modes are essentially associated with a tangential motion of the carbon atoms (Kuzmany et al. 1995 and 2000). The most characteristic vibrational mode is the pentagonal "pinch" mode at 1427 cm^{-1}. When C_{60} is cooled to -13°C a phase transition occurs to an ordered state referred as "ratchet phase" (Graja et al. 1995). On further cooling the C_{60} crystals between -123°C to -183°C, a glass transition can be observed due to the fact that C_{60} molecules shuffle into two nearly degenerate orientations. On further decreasing temperature, the population of C_{60} molecules with energetically less favorable orientation decrease but not vanish completely. Indeed, even below -183°C about 17% of the C_{60} is found to be frozen in the energetically less favorable orientation leading to a glass-like behaviour (Graja et al. 1995; Kuzmany et al. 1995, 2000). Such transitions can be followed by plotting the relative intensity or the peak height of the 4 infrared absorption bands as function of the temperature (Kamaras et al. 1993; Graja et al. 1995).

In Fig. 1 we report the FT-IR spectra of C_{60} measured with our apparatus at +250°C, +75°C and at -180°C. At low temperature the infrared spectrum results better resolved, this well known phenomenon of band sharpening and increase in intensity can be better appreciated in Fig. 2 where the synthetic spectrum derived from the subtraction of the low temperature (-180°C) spectrum of C_{60} from that recorded at + 250°C is reported. The peaks pointing downward are due to the low temperature spectrum: 6.988 μm, 8.443 μm, 17.316 μm, 19.044 μm. The peaks pointing upward are due to the high temperature spectrum: 6.946 and 7.052 μm, 8.422 and 8.506 μm, 17.210 and 17.484 μm, 18.833 and 19.191 μm. It is evident from the spectrum in Fig. 1 that the bandwidth was larger at higher temperature and became narrower at low temperature. This behavior of the C_{60} infrared absorption spectrum with respect to temperature was already reported and analyzed by Frum et al. 1991 and by Nemes et al. 1994.

An additional feature of the low temperature spectra of C_{60} is the shift of the position of the infrared bands. This is illustrated in Fig.3 on the $F_{1u}(3)$ band of C_{60}. When the temperature decreases from +250°C to -180°C the absorption peak originally located at 1178 cm^{-1} shifts to a higher frequency i.e. 1182 cm^{-1}. Additionally, the bandwidth is reduced from 8.95 cm^{-1} to 7.97 cm^{-1} and the peak area passes from 2.275 to 2.400, since at lower temperature there is a sharpening of the absorption band but also an increase in intensity. It is known that even in the solid state the C_{60} molecules rotate at high temperature and there is interaction between adjacent molecules; the coupling of the vibration with the diffuse rotation is the cause of the band broadening. Decreasing the temperature, the rotation is inhibited and also there is a decay of the vibration into a lower lying optical mode and a lattice mode (Kuzmany et al. 2000).

The infrared peak position at 0 K (-273°C) has been determined simply by extrapolation of the peak position data measured in the range from +250°C to -180°C. This is a relevant information for the search of the fullerene infrared "signature" in the interstellar or circumstellar medium. The resulting data are reported in Table 1. Fig. 4 illustrates the procedure for the pentagonal "pinch" vibrational

mode of C_{60}: the peak position at three (or more) different temperatures are plotted against temperature and the resulting linear dependence is employed to determine the infrared absorption peak position of C_{60} at 0 K. As shown in Fig. 4 the expected peak position of the pentagonal "pinch" vibrational mode of C_{60} at 0 K is 1430.9 cm^{-1}, about 9.7 cm^{-1} higher frequency than the band position at +250°C. In Table 1 are reported the peak position of the 4 absorption bands of C_{60} extrapolated to 0 K. All our C_{60} infrared measurements were made in a KBr matrix.

TABLE 1 - Summary of C_{60} infrared band position and width (full width half maximum in parenthesis) all data in cm^{-1}

-273°C (**) gas phase extrapol. to 0 K	-273°C (*) KBr matrix extrapol. to 0 K	-190°C (**) Ar matrix measured	-180°C (*) KBr matrix measured	+250°C (*) KBr matrix measured	+792°C (**) gas phase measured	810°C (***) gas phase measured	810°C (*) KBr matrix extrapol. to 1083 K
1435.5	1430.9	1431.9 (4)	1428.9 (10.8)	1421.2 (10.7)	1406.9 (12)	1407.2 (13.5)	1411.7
1190.7	1183.0	1184.8 (2)	1182.3 (7.9)	1178.2 (8.9)	1169.1 (13)	1165.8	1173.4
574.4	576.8	579.3 (2)	574.7 (6.9)	572.7 (10.0)	570.3 (13)	570.0 (13.7)	570.0
531.2	525.0	530.1 (1)	524.0 (6.9)	524.0 (8.8)	527.1 (11)	527.5 (11.6)	

(*) This work
(**) Frum et al. 1991
(***) Nemes et al. 1994

In Table 1 the infrared peak positions of C_{60} measured in other environments are also reported. It is interesting to compare the data taken at -190°C in an Ar matrix with our data recorded at -180°C in the KBr matrix. The four infrared band frequencies of C_{60} are shifted toward higher wavenumbers from 2.5 to 6.1 cm^{-1} for the C_{60} sample embedded in Ar matrix. This suggests a lower interaction with the Ar matrix in comparison with the sample in the KBr matrix but also a lower degree of freedom of the molecules and perhaps a much more C_{60}-C_{60} lattice interaction. Furthermore, also the values of full-width at half maximum (fwhm) of the absorption bands reported in parenthesis in Table 1 show significant differences, being significantly smaller for the C_{60} sample in Ar matrix, in line with the explanation already given for the frequency shift.

Frum et al. 1991 as well as Nemes et al. 1994 have studied the gas phase spectra of C_{60} above +800°C. Their data are reported in Table 1. At +800°C is not surprising to find fwhm values above 10 cm^{-1} which can be attributed to the high rotational freedom of the molecules at this temperature. It is interesting to note that fwhms of the same order of magnitude were found in our infrared study on C_{60} embedded in a KBr matrix and heated at +250°C. By extrapolating the vibrational frequencies measured at +250°C in KBr to +810°C using the following equations (T in K):

$$\nu_{F1u(4)} = -0.0177\ T + 1430.9 \qquad \text{[eq.1]}$$

$$\nu_{F1u(3)} = -0.00884\ T + 1183.0 \qquad \text{[eq.2]}$$

$$\nu_{F1u(2)} = -0.0063\ T + 576.8 \qquad \text{[eq.3]}$$

the expected infrared frequencies at 810°C in a hypothetical gas phase result: 570.0, 1173.4 and 1411.7 cm^{-1}. By comparing these values with the gas phase values reported in Table 1, it can be observed that at high temperature the matrix effect of KBr affects only the bands at 1173.5 and 1412.0 cm^{-1} causing in comparison to the gas phase bands a shift to higher frequencies of 4.5 and 7.6 cm^{-1} respectively. The band at 570 cm^{-1} appears independent from temperature.

Given the astrochemical interest of vibrational frequencies at very low temperatures, the vibrational frequencies of the gas phase spectra of C_{60} taken in the range of temperature comprised between +606°C and +939°C were extrapolated by Nemes et al. (1994) to derive the theoretical position of these bands at 0 K. Their results are listed in Table 1 and the C_{60} infrared bands positions are expected at and 531.2, 574.4, 1190.7 and 1435.5 cm^{-1}. Table 1 also shows the extrapolation to 0 K of the C_{60} infrared absorption bands measured in a KBr matrix which results: 525.0, 576.8, 1183.0 and 1430.9 cm^{-1} in reasonable agreement with the data obtained from gas phase measurements.

3.2 The low temperature and high temperature gas phase FT-IR spectra of C_{70} fullerene

In C_{70}, because of its lower D_{5h} symmetry, there are five kinds of non-equivalent atomic sites and eight kinds of non-equivalent bonds. This means that the number of normal vibrations is larger for C_{70} than for C_{60}. Although there are now 204 vibrational degrees of freedom for the 70-atom molecule, the symmetry of C_{70} gives rise to a number of degenerate modes so that only 122 modes are expected. Of these 31 are infrared-active and 53 are Raman-active (Kuzmany et al. 1995 and 2000).

Owing to the elongated form and reduced symmetry of the C_{70} molecule, the orientational transition and crystal phases are more complicated than in C_{60}. A variety of measurements have shown that the C_{70} crystal can be prepared in either f.c.c. or hexagonal, close-packed h.c.p. form. Since the two forms are almost isoenergetic they can co-exist under certain conditions. The transition from a fully disordered phase to a partially ordered phase occurs at +64°C (337 K) but the low temperature ordered phase can be reached at +3°C (276 K) (Varma et al. 1993). Another transition in C_{70} occurs at -73°C (200 K).

In Fig. 5 two FT-IR spectra of C_{70} recorded respectively at -180°C and at +250°C as in the previous case of C_{60} are reported. In the wavelength (μm) scale of the abscissa it is difficult to appreciate the band shift due to temperature change occurred in C_{70} embedded in KBr. Therefore, Fig. 6 and 7 show the details of the spectra in wavenumbers putting in evidence the small band shift measured at the two temperatures employed.

TABLE 2 - Summary of C_{70} infrared band position and width (full width and half maximum in parenthesis) in cm^{-1}

-273°C (*) KBr matrix extrap to 0 K	-273°C (**) gas phase extrap to 0 K	-180°C (*) KBr matrix	+250°C (*) KBr matrix	+810°C KBr matrix extrap. to +810°C	+810°C (**) gas phase	+810°C (**) gas phase emission
1429.6	1432.0	1428.6	1424.2	1418.5	1411.8 (18.2)	1411.8
1413.5		1412.8	1409.6	1405.5		
1322.9		1321.5	1315.1	1306.8		
1133.5	1144.1	1132.5	1128.1	1122.4	1121.7 (14.7)	1122.2
1085.8	1099.6	1085.0	1081.2	1076.3	1077	1077.2
793.5	793.0	793.3	792.2	790.7		793.3
724.6		724.5	724.0	723.3		
		671.0	671.0			
	638.0	639.5	639.5			638.5
	583.1	574.5	574.4		574.9	575.3
	567.7	562.9	562.9		556.9	553.3
534.0	545.0	533.5	531.4	528.6	527.6 (10.0)	528.2
457.2		456.9	455.3	453.2		

(*) This work

(**) Nemes et al. 1994

As already observed for C_{60}, by passing from high (+250°C) to low temperatures (-180°C) there is a systematic shift of the vibrational bands to higher frequencies although there are also bands which appear completely insensitive to the temperature change. For C_{60} an example of infrared band not sensitive to temperature change, at least in a KBr matrix, is that at 524 cm^{-1} (see Table 1). As shown in Table 2, a similar phenomenon can be observed also in the infrared spectra of C_{70} where a series of vibrational absorption bands are quite insensitive to the temperature change of the sample in KBr matrix. However, there are also other vibrational bands of C_{70} whose frequency is dependent on temperature and their positions at 0 K were extrapolated. The results of such extrapolations are reported in Table 2 in comparison with the extrapolation of C_{70} absorption bands from gas phase infrared spectra by Nemes et al. (1994). As expected in both cases the temperature-sensitive bands tend to shift to the highest possible frequencies and the shift appears more pronounced with the extrapolation from the gas phase data rather than for the data taken in KBr and this is certainly due to a matrix effect.

The infrared vibrational frequencies of C_{70} taken in a KBr matrix in the temperature range between -180°C to +250°C were also extrapolated to very high temperature, i.e. +810°C and compared with the gas phase spectrum of C_{70} (Nemes et al. 1994). We found good agreement. Another interesting aspect reported in Table 2 is the remarkable coincidence of the positions of the emission and absorption infrared bands of C_{70} in gas phase (Nemes et al. 1994).

3.3 – The molar absorptivity or molar extinction coefficient of C_{60} and C_{70} at ambient temperature

In the previous sections the dependence on temperature of the positions and widths of the infrared absorption bands of C_{60} and C_{70} has been determined. However, it has not been reported neither the molar extinction coefficient of each absorption band nor the integrated molar band intensity and their dependence from temperature.
If I_0 is the intensity (radiant power) of the monochromatic radiation entering a sample and I the intensity transmitted by the sample, then the logarithm of the ratio I_0/I is the absorbance A (Colthup et al. 1990):

$$A = \mathrm{Log}\,[I_0/I] = \varepsilon bc \qquad \text{[eq.4]}$$

According to the Lambert and Beer law, the absorbance is directly proportional to the thickness b (or optical path length) and the concentration c of the absorbing molecules in the infrared beam. As shown in eq. 4, the proportionality constant linking absorbance with the optical path length and with concentration is ε, known as molar absorptivity or more commonly known in the literature as molar extinction coefficient whose typical physical dimensions are $L \bullet cm^{-1} \bullet mol^{-1}$ (Colthup et al. 1990).
The determination of the molar extinction coefficient at a given wavenumber ε_λ was made through the equation using the absorbance A_λ at a given wavenumber:

$$\varepsilon_\lambda = A_\lambda (bc)^{-1} \qquad \text{[eq.5]}$$

The value of $(bc)^{-1}$ was then determined for both C_{60} and C_{70} using the experimental parameters reported in the experimental section and a KBr density of 2.753 g/cm^3. The $(b^{-1}c^{-1})$ values found were respectively 410.9 $L \bullet cm^{-1} \bullet mol^{-1}$ for C_{60} and 437.8 $L \bullet cm^{-1} \bullet mol^{-1}$ for C_{70}.
From the infrared spectrum of C_{60} the absorbance values A_λ have been determined using the Ominc software of the infrared spectrometer. In Table 3 we summarize the results of such measurements and report the molar extinction coefficient values ε_λ calculated according to eq. 5.

TABLE 3 - C_{60} INFRARED MOLAR EXTINCTION COEFFICIENT AND INTEGRATED MOLAR ABSORPTIVITY

wavenumber cm^{-1}	wavelength μm	Mol. Extinc. Coeff. $[\varepsilon_\lambda]$ L cm^{-1} mol^{-1}	$[\varepsilon_\lambda]$ Relative Intensity	Integrated mol absorptivity $[\Psi]$ Km mol^{-1}	$[\Psi]$ Relative Intensity
1427	7.0	63.1	26.9	10.4	34.4
1180	8.5	61.5	26,2	9.4	31.1
574	17.4	100.6	43.0	16.2	53.6
524	19.1	234,2	100	30.2	100

The ε_λ values reported in Table 3 are the average of 5 different measurements made on two different samples at room temperature. The statistical treatment of the experimental data, consisting in the calculation of the standard deviation (σ) and in the derivation of the resulting $\pm 2\sigma$ values shows that the ε_λ values reported in Table 3 have an uncertainty ±10% .
Table 3 reports also the relative intensity of the ε_λ values taking as 100 the most intense $F_{1u}(1)$ infrared mode at frequency 524 cm^{-1}. Such values should be compared with those reported by Fabian (1996): for the infrared absorption bands at 524, 574, 1180 and 1427 cm^{-1} ($F_{1u}(i)$, i=1,2,3,4) the relative intensity are 100, 48, 45 and 37.8 respectively. Thus only the relative intensity or the band ratio A_{574}/A_{524} reported by Fabian (1996) is in agreement with the results reported in Table 1 for the relative intensity of the ε_λ values. For the other bands at 1427 and 1180 cm^{-1} the relative intensity found in the present work appear smaller than that reported by Fabian (1996). However, another work (Martin et al. 1993) reports completely different relative intensity of the $F_{1u}(i)$ vibration modes: 100, 40, 9 and 5 showing that the bands at higher frequencies are more affected than others by the way the height of the peak is measured, the spectrometer resolution, the type of sample under study (e.g. thin solid film, KBr pellet, etc…). To avoid such sources of variability and uncertainty, the integrated molar absorptivity has been determined, as detailed in the next section.

TABLE 4 - C_{70} INFRARED MOLAR EXTINCTION COEFFICIENT AND INTEGRATED MOLAR ABSORPTIVITY

wavenumber cm^{-1}	wavelength μm	Mol. Extinc. Coeff. $[\varepsilon_\lambda]$ L cm^{-1} mol^{-1}	$[\varepsilon_\lambda]$ Relative Intensity	Integrated mol absorptivity $[\Psi]$ Km mol^{-1}	$[\Psi]$ Relative Intensity
1427+1413	7.0+7.1			**89.5**	
1427	7.0	**207.9**	100	**22.5**	100
1413	7.1	**29.2**	14.0	**2.2**	10.0
1132	8.8	**57.3**	27.6	**7.0**	31.3
792	12.6	**68.7**	33.1	**7.6**	33.8
723	13.8	**18.5**	8.9	**1.5**	6.9
671	14.9	**129.0**	62.0	**15.3**	68.0
640	15.6	**77.6**	37.3	**22.8**	101.2
574	17.4	**142.9**	68.7	**10.6**	47.0
565	17.7	**44.5**	21.4	**4.2**	18.8
532	18.8	**182.6**	87.8	**26.4**	117.2
455	22.0	**72.1**	34.7	**5.8**	25.6

In Table 4 are reported the molar extinction coefficient ε_λ of the most important infrared absorption bands of C_{70}. The values reported result from the average of three distinct measurements. The same statistical treatment of the data described previously for C_{60} has been adopted for C_{70} and again, an uncertainty of about ±10% was determined. In Table 4 the ε_λ values were also transformed into the relative intensity taking as 100 the most intense band at 1427 cm^{-1}. There is a reasonable agreement between the relative intensity data measured in the present work and values reported in the literature (Von Czarnowski, Meiwes-Broer, 1995).

3.4 – The integrated band intensities of C_{60} and C_{70} at ambient temperature

The peak height measurements which correspond to the absorbance A as shown by eq.4, are sensitive to changes in the resolution of the spectrometers used and can vary from instrument to instrument (Colthup et al. 1990). The integrated band intensity corresponds to the measurement of the total intensity area associated to a given absorption band. Such measurement is much less sensitive to instrumental resolution than the peak height measurement. The Omnic software of our FTIR spectrometer is able to measure either the height of a given absorption band or the total area under the same band, in both cases subtracting automatically the baseline. Thus, the integrated intensity has been determined in the infrared spectra of C_{60} and C_{70} at ambient temperature.
The integrated intensity can be expressed as the integrated absorptivity Ψ defined as follows (Colthup et al. 1990):

$$\Psi = \int \varepsilon_\lambda \, d\lambda \qquad \text{[eq.6]}$$

where λ is the wavenumber and ε_λ is the absorptivity measured with a spectrometer with unlimited resolution, integrated over the whole band. In practice, by substituting eq. 2 in eq. 3 we get (Colthup et al. 1990):

$$\Psi = (bc)^{-1} \int A_\lambda \, d\lambda \qquad \text{[eq.7]}$$

If the optical path length b is measured in cm and the concentration is measured in mol/cm^3 and the spectrum is plotted using the wavenumber scale in cm^{-1} versus the absorbance A_λ, then the integrated absorbance Ψ is expressed in $cm \bullet mol^{-1}$ or 10^{-5} $Km \bullet mol^{-1}$ (Colthup et al. 1990).
In these units, Ψ is related to the square of the dipole moment change with respect to the normal coordinates $(\partial\mu/\partial Q)^2$ by the relationship (Colthup et al. 1990):

$$\Psi = [\pi N/3C^2 \, (Ln10)] \, (\partial\mu/\partial Q)^2 = 304.75 \, (\partial\mu/\partial Q)^2 \; cm \bullet mol^{-1} \qquad \text{[eq.8]}$$

with N the Avogadro's number, C the velocity of light in cm/sec and $(\partial\mu/\partial Q)$ in (esu cm)/(cm $g^{1/2}$).
With these premises, the integrated molar absorptivity of all the infrared absorption bands of C_{60} have been determined at ambient temperature and are shown in Table 3 together with the relative intensity. As expected the uncertainty of the data reported in Table 3 and pertaining the Ψ values of C_{60} are in the range of ±8%. Furthermore, a reasonable agreement can be found in the relative intensity of the bands calculated from the ε_λ values or from the Ψ values.
In Table 4 we report the integrated molar absorptivities of C_{70} determined at room temperature in KBr. Only the most intense bands of the C_{70} infrared spectrum have been selected for the determination of Ψ. The infrared bands at 1427 and 1413 cm^{-1} appear as a doublet with the first band more intense than the other. The absorbance peak integration was conducted in two modes: either by including both bands in a unique integral and the result of such integration is shown as

1427+1413 in Table 4 or by integrating separately the two bands and in such a case two separate Ψ values are reported in Table 4.

Since the integration limits of the absorption bands affect Ψ, in Table 5 we report the integration ranges adopted for each band.

TABLE 5 - INTEGRATION RANGES FOR THE DETERMINATION OF THE INFRARED MOLAR ABSORPTIVITY

wavenumber cm^{-1}	Integration ranges for Ψ determination cm^{-1}
C_{60}	C_{60}
1427	1434-1375
1180	1190-1136
574	586-534
524	534-495
C_{70}	C_{70}
1427+1413	1438-1338
1427	1438-1417
1413	1417-1400
1132	1142-1109
792	800-771
723	733-713
671	679-648
640	648-582
574	582-569
565	569-542
532	540-495
455	463-442

3.6 – About the temperature dependence of the integrated band intensities of C_{60} and C_{70}

The quantitative determination of fullerenes in space requires also knowledge on the dependence of ε and Ψ with temperature. As discussed in the previous section, the integrated absorptivity Ψ is more reliable than the molar extinction coefficient ε for a number of reasons. Therefore the dependence of Ψ was determined as reported in the experimental sections 2.2 and 2.3. Fig. 8 shows that the dependence of Ψ with the absolute temperature is linear for three C_{60} absorption bands and increases by decreasing the temperature. Instead the C_{60} infrared absorption band at about 1180 cm^{-1} appears much less dependent from temperature than the other bands. In all cases the experimental data were extrapolated to -273°C (0 K) and the resulting equations valid in a wide range of temperatures for each C_{60} fullerene absorption band were determined with a high degree of correlation factor (R^2) with the experimental data. In fact, the integrated absorptivity Ψ(T) expressed in Km/mol of each C_{60} infrared absorption frequency can be described by the following linear equations (T is absolute temperature in Kelvin):

at 524 cm^{-1}: $\Psi_{524} = (-0.0134\ T + 34.847)$ with $R^2 = 0.9865$ [eq. 9]

at 574 cm^{-1} : $\Psi_{574} = (-0.0166\ T + 22.891)$ with $R^2 = 0.9666$ [eq. 10]

at 1180 cm^{-1}: $\Psi_{1180} = (-0.0184\ T + 17.415)$ with $R^2 = 0.9148$ [eq. 11]

at 1427 cm^{-1}: $\Psi_{1427} = (-0.0032\ T + 10.366)$ with $R^2 = 0.9460$ [eq. 12]

In Table 6 we report the Ψ experimental data at different temperatures from which the eq. 9-12 have been derived.

Cami et al. (2010) have used an integrated molar absorptivity of 25 Km•mol^{-1} for the C_{60} infrared band at 8.5 μm (which corresponds to the frequency of 1180 cm^{-1}) in the quantitative estimation of C_{60} around the young planetary nebula Tc1. However, our measurement reported in Table 3 shows that Ψ_{1180} = 9.8 Km•mol^{-1}, consequently the value used by Cami et al. (2010) may appear at a first sight as source of an overestimation. However our data on Ψ of C_{60} reported in Table 3 were determined only at room temperatures while the Ψ_{1180} data used by Cami et al. (2010) derived from a work where C_{60} was frozen in a cryogenic hydrogen matrix (Sogoshi et al. 2000). Using eq. 11, the maximum Ψ_{1180} value is reached at 0 K and corresponds to 17.415 Km/mol. Thus, the slight overestimation of fullerene concentration reported by Cami is confirmed.
Furthermore, the Ψ of the other C_{60} absorption bands used by Cami et al. (2010) were scaled using the relative intensity of the absorption bands measured at room temperature taken from Fabian (1996) assuming that the relative intensity remains unchanged with temperature. The equations 9-11 show that the relative intensity of the absorption bands of C_{60} may vary at different temperatures and the band at 1180 cm^{-1} is the less sensitive to temperature, so it is less useful for the determination of the relative intensity at different temperatures.
The dependence of integrated absorptivity Ψ with temperature was determined also in the case of C_{70} fullerene. The infrared spectrum of C_{70} is more complex than that of C_{60} and more rich of absorption bands. For the determination of the Ψ(T) only some bands of the C_{70} spectrum were followed in a wide range of temperature comprised between -180°C and +250°C. The bands selected for the determination of Ψ(T) were those showing a linear dependence of Ψ with the temperature change with a high correlation factor R^2. The linear equations describing the dependence of Ψ of the selected infrared C_{70} bands with temperature are derived from the graphs of Fig. 9 and 10 (T is absolute temperature in Kelvin):

at 532 cm^{-1}: $\Psi_{532} = (-0.0127\ T + 30.835)$ with $R^2 = 0.9813$ [eq. 13]

at 565 cm^{-1}: $\Psi_{565} = (-0.0115\ T + 8.493)$ with $R^2 = 0.9686$ [eq. 14]

at 576+563 cm^{-1}: $\Psi_{576+563} = (-0.0241\ T + 40.71)$ with $R^2 = 0.9992$ [eq. 15]

at 640 cm^{-1}: $\Psi_{640} = (-0.0499\ T + 39.821)$ with $R^2 = 0.9983$ [eq. 16]

at 671 cm^{-1}: $\Psi_{671} = (-0.0089\ T + 17.607)$ with $R^2 = 0.9421$ [eq. 17]

at 1132 cm^{-1}: $\Psi_{1132} = (-0.0066\ T + 8.943)$ with $R^2 = 0.961$ [eq. 18]

at 1427+1413 cm^{-1}: $\Psi_{1427+1413} = (-0.0114\ T + 73.085)$ with $R^2 = 0.8678$ [eq. 19]

All the selected infrared absorption bands reported in eq. 13-19 show a high degree of correlation factor R^2 and for T= 0 K the extrapolated value of Ψ at absolute zero (expressed in Km/mol) can be obtained. As shown in Fig. 6, the band at about 1427 cm^{-1} occurs with a shoulder which becomes a sub-band at lower temperatures located at about 1413 cm^{-1}; the $\Psi_{1427+1413}$ value reported in eq. 18

was determined on the entire absorption band including also the sub-band. Similarly, also in the case of the determination of Ψ of the infrared absorption band at about 576 cm^{-1} (see Fig. 7), the sub-band at 563 cm^{-1} has been included so that the $\Psi_{576+563}$ trend is described by eq. 14.
Other C_{70} infrared absorption bands whose Ψ is not reported in the equations 13-19 are the bands at 1413, 792, 723, 574 and 455 cm^{-1} which show a poor correlation coefficient R^2 and/or a scarce dependence from temperature in their Ψ values. However also the Ψ values of these bands are reported in Table 7.

Conclusions

The infrared absorption spectra of C_{60} and C_{70} were recorded in a KBr matrix in the temperature range comprised between -180°C and +250°C. The experimental data, in terms of infrared absorption band position and infrared band shift as function of temperature were extrapolated to absolute zero and above +800°C. The results of such extrapolations recorded in KBr matrix were compared with the fullerenes infrared spectra recorded in other inert matrices or in the gas phase.
The entity of the matrix effect exerted by KBr has been quantified both at -273°C and it has been found that at +800°C the matrix effect of KBr becomes negligible.
Furthermore, the molar extinction coefficient ε and the integrated molar absorptivity of the infrared absorption bands of C_{60} and C_{70} fullerenes were determined at ambient temperature. The integrated molar absorptivity Ψ is a more reliable constant than ε and hence the dependence of Ψ with temperature was measured in the range comprised between -180°C and +250°C and extrapolated to -273°C. Equations for the calculation of the integrated molar absorptivity Ψ of the most important infrared absorption bands of C_{60} and C_{70} from -273°C to >250°C were determined.

Acknowledgements

The present research work has been supported by grant AYA2007-64748 Expte. NG-014-10 of the Spanish Ministerio de Ciencia e Innovacion.

References

Bell, M.B., Feldman, P.A., Travers, M.J., McCarthy, M.C., Gottlieb, C.A., Thaddeus, P., 1997, Astrophys. J. Lett. 483, L61.

Cami, J., Bernard-Salas, J., Peeters, E., Malek, S. E., 2010, Science, 329, 1180.

Cataldo, F., Iglesias-Groth, S., Manchado, A., 2010, Fullerenes Nanot. Carbon Nanostruct. 18, 224.

Cataldo, F., Iglesias-Groth, S. (eds.), 2010, Fulleranes: The Hydrogenated Fullerenes. Springer, Dordrecht, The Netherlands.

Cataldo, F., Iglesias-Groth, S., 2009, Monthly Not. Roy. Astronom. Soc., 400, 291.

Cataldo, F., Strazzulla, G., Iglesias-Groth, S., 2009, Monthly Not. Roy. Astronom. Soc., 394, 615.

Cataldo, F., 2003, Fullerenes Nanot. Carbon Nanostruct. 11, 295.

Clayton, G. C., Kelly, D. M., Lacy, J. H., Little-Marenin, I. R., Feldman, P.A., Bernath, P. F., 1995,

Astronom. J. 109, 2096.

Colthup, N.B., Daly, L.H., Wiberley, S.E., 1990, Introduction to Infrared and Raman Spectroscopy. 3rd Edition. Academic Press, San Diego, p. 100-103.

Ehrenfreund, P., Foing, B. H. 2010, Science, 329, 1159.

Fabian, J., 1996, Phys. Rev. B, 53, 13864.

Foing, B.H., Ehrenfreund, P., 1994, Nature 369, 296.

Frum, C.I., Engleman, R., Hedderich, H.G., Bernath, P.F., Lamb, L.D., Huffman, D.R. (1991). Chem. Phys. Lett. 176: 504.

Goeres, A., Sedlmayr, E., 1993, Fullerenes Nanot. Carbon Nanostruct. 1, 563.

Garcia-Hernandez, D.A., Manchado, A., Garcıa-Lario, P., Stanghellini, L., Villaver, E., Shaw, R.A., Szczerba, R., Perea-Calderon, J.V., 2010, Astrophys. J., *accepted for publication.*

Graja, A., Swietlik, R., 1995, Synth. Metals, 70, 1417.

Hare, J. P., Kroto H. W., 1992, Acc. Chem. Res. 25, 106.

Iglesias-Groth, S., 2004, Astrophys. J. 608, L37

Iglesias-Groth, S., 2006, Monthly Not. Roy. Astronom. Soc., 368, 1925.

Iglesias-Groth, S., 2007, Astrophys. J., 661, L167.

Iglesias-Groth, S., Manchado, A., Rebolo, R., González Hernández, J. I., García-Hernández, D. A., Lambert, D. L., 2010, Monthly Not. Roy. Astronom. Soc., 407, 2157.

Kamaras, K., Akselrod, L., Roth, S., Mittelbach, A., Honle, W., Von Schnering H.G., 1993, Chem. Phys. Lett. 214, 338.

Kroto, H.W., 1988, Science 242, 1139.

Kroto, H.W., 1992, Angew. Chem. Int. Ed. Engl. 31, 111.

Kuzmany, H., Winkler, R., Pichler , R., 1995, J. Phys. Condens. Matter , 7, 6601.

Kuzmany, H., Winter, J., 2000, "Vibrational properties of fullerenes and fullerides" in The Physics of Fullerenes and Related Materials. Edited by Andreoni W., World Scientific, Singapore, p.208.

Martin, M., Koller, D., Mihaly, L., 1993, Phys. Rev. B, 47, 14607.

Nemes, L., Ram, R.S., Bernath, P.F., Tinker, F.A., Zumwalt, M.C., Lamb, L.D., Huffman, D.R., 1994, Chem. Phys. Lett. 218, 295.

Nuccitelli, D., Richter, M. J., McCall, B. J., 2005, IAU Symposium 231, poster session 2: poster 42.

Sellgren, K., Werner, M.W., Ingalls, J.G., Smith, J.D.T., Carleton, T.M., Joblin, C., 2010, Astrophys. J. Lett. 722, L54.

Sellgren, K., Werner, M. W., Ingalls, J. G., 2009, Bull. Amer. Astronom. Soc. 41, 664.

Sogoshi, N., Kato, Y., Wakabayashi, T., Momose, T., Tam, S., DeRose, M.E., Fajardo, M.E., 2000, J. Phys. Chem. A, 104, 3733.

Varma, V., Sashandri, R., Govindaraj, A., Sood, A.K., Rao, C.N.R., 1993, Chem. Phys. Lett., 203, 54.

Von Czarnowski, A., Meiwes-Broer, K.H., 1995, Chem. Phys. Lett. 246, 321.

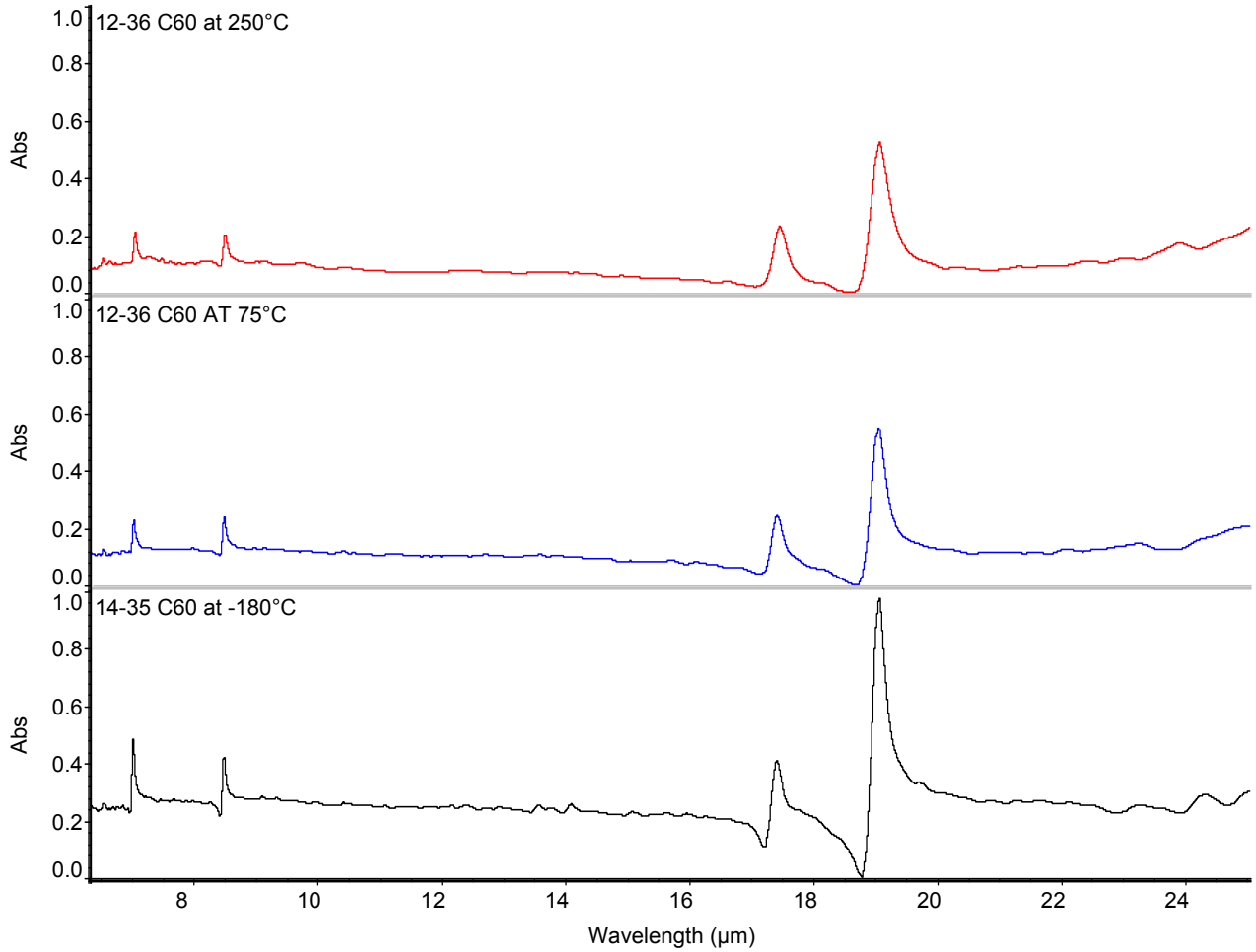

Fig. 1 - FT-IR spectra of C_{60} in KBr taken respectively (from top to bottom) at +250°C, +75°C and at -180°C.

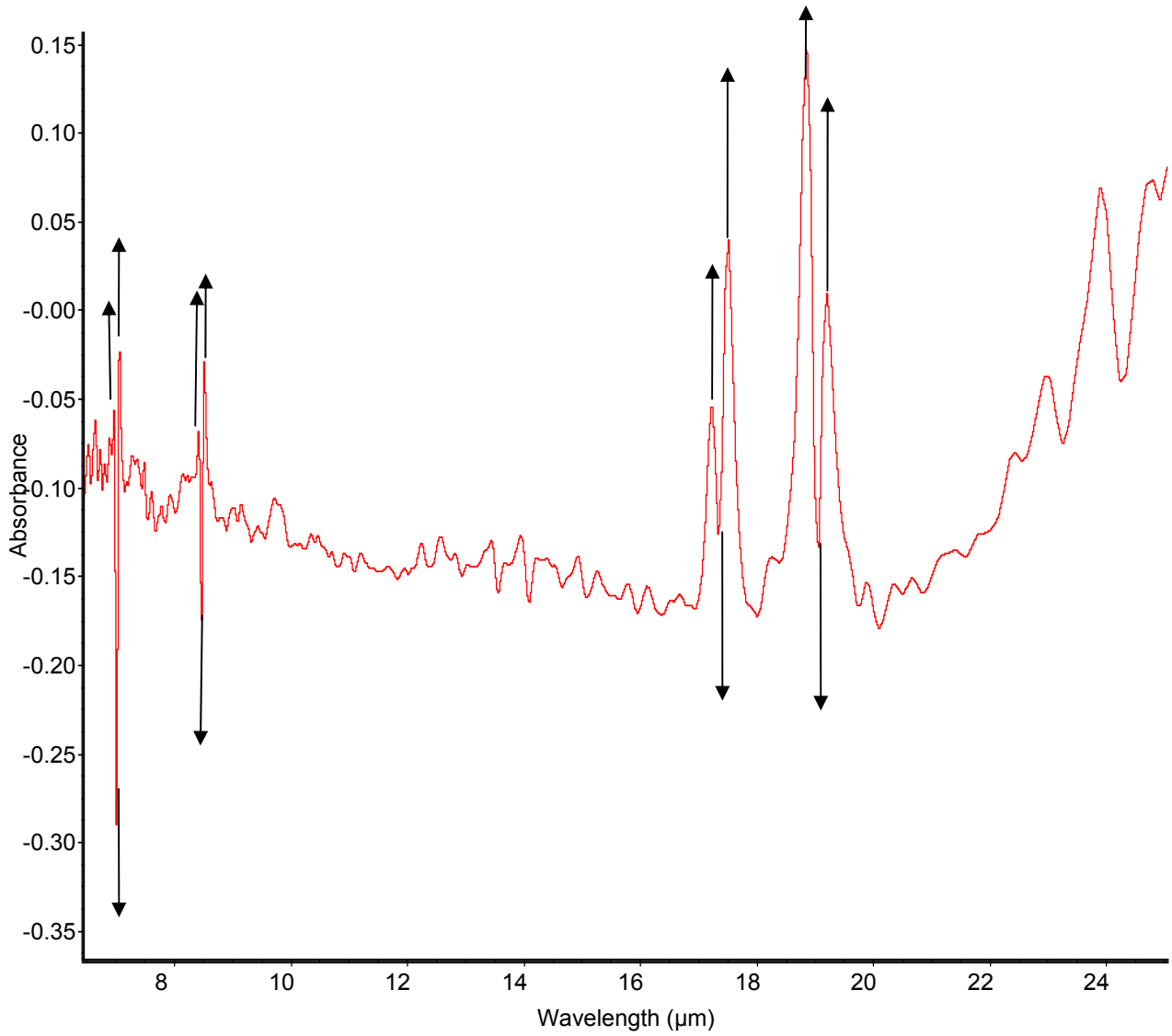

Fig. 2 – Spectrum derived from the subtraction of the low temperature (-180°C) spectrum of C_{60} from that recorded at + 250°C. The peaks pointing downward (marked with arrows pointing downward) are due to the low temperature spectrum: 6.988 µm, 8.443 µm, 17.316 µm, 19.044 µm. The peaks pointing upward are due to the high temperature spectrum: 6.946 and 7.052 µm, 8.422 and 8.506 µm, 17.210 and 17.484 µm, 18.833 and 19.191 µm (marked with arrows pointing upward). It is evident from such difference spectrum that the bandwidth was larger at higher temperature and became narrower at low temperature.

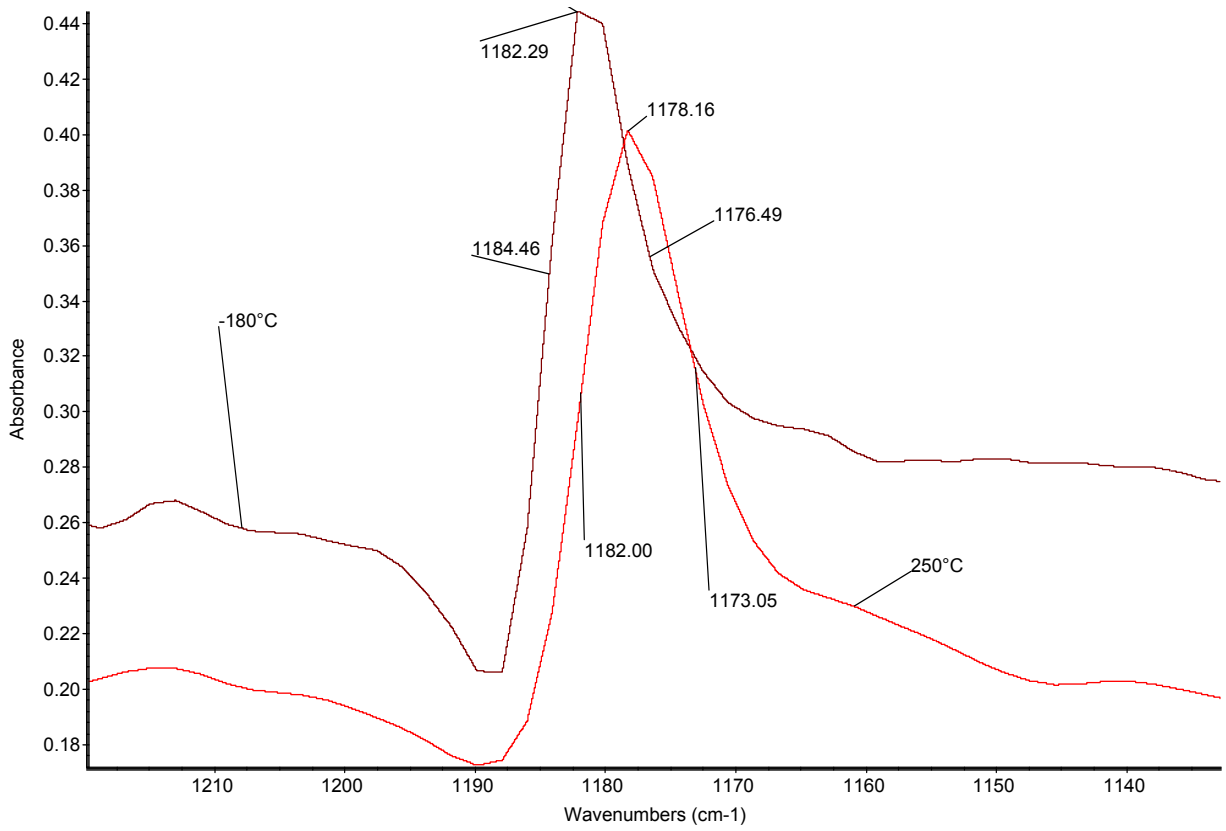

Fig. 3 – FT-IR spectra of C_{60} (in KBr). On lowering the temperature from +250°C to -180°C the absorption peak originally located at 1178 cm^{-1} shifts at higher frequencies i.e. 1182 cm^{-1}. Additionally, the bandwidth is reduced from 8.95 cm^{-1} to 7.97 cm^{-1} respectively from +250°C to -180°C and the peak area passes from 2.275 to 2.400 since at lower temperature there is a sharpening of the absorption band but also an increase in intensity.

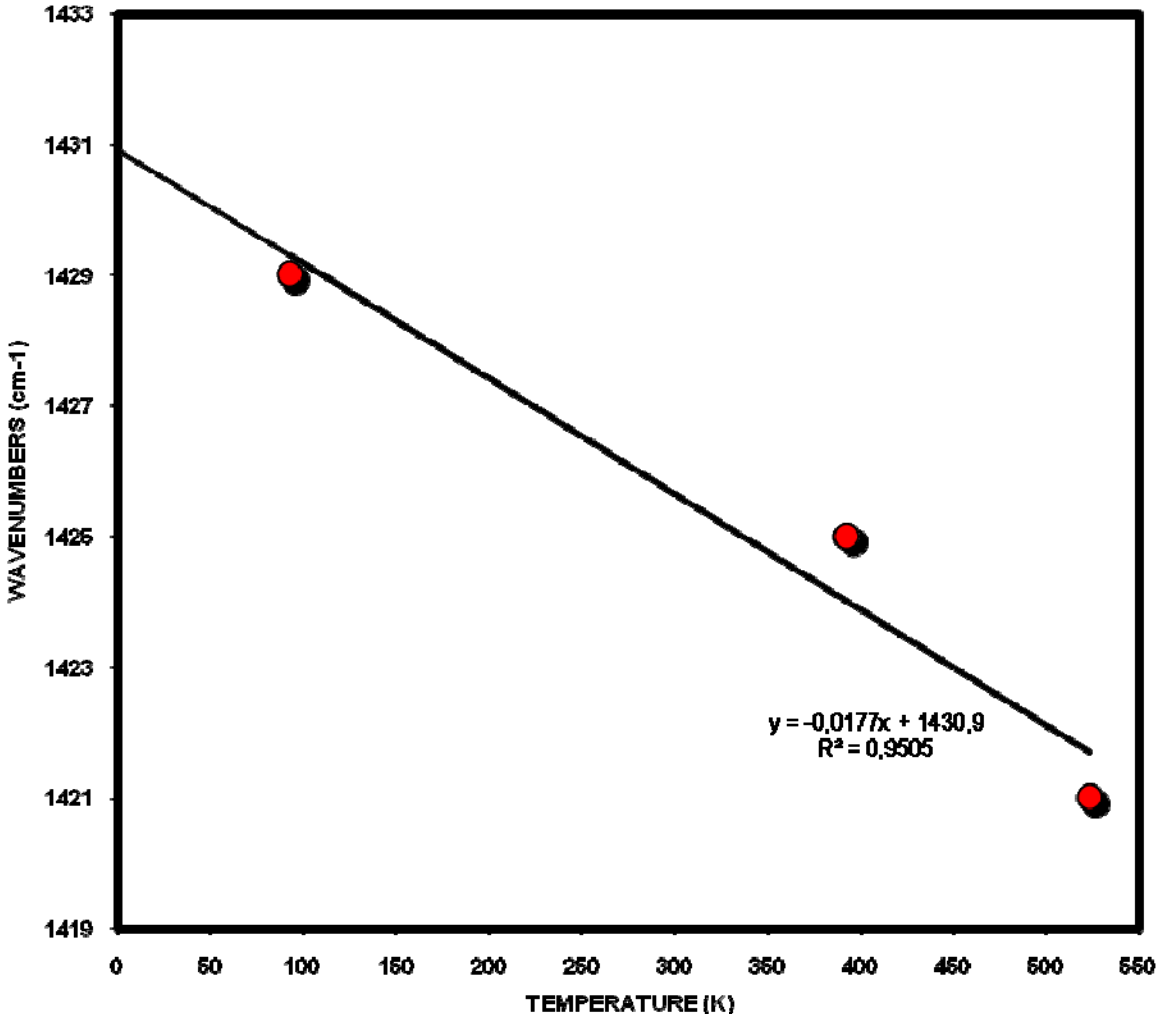

Fig. 4 – Extrapolation to 0 K of a C_{60} infrared absorption band position. This is the case of the $F_{1u}(4)$ band, the pentagonal "pinch" mode. The intercept at 0 K occurs at 1430,9 cm^{-1}.

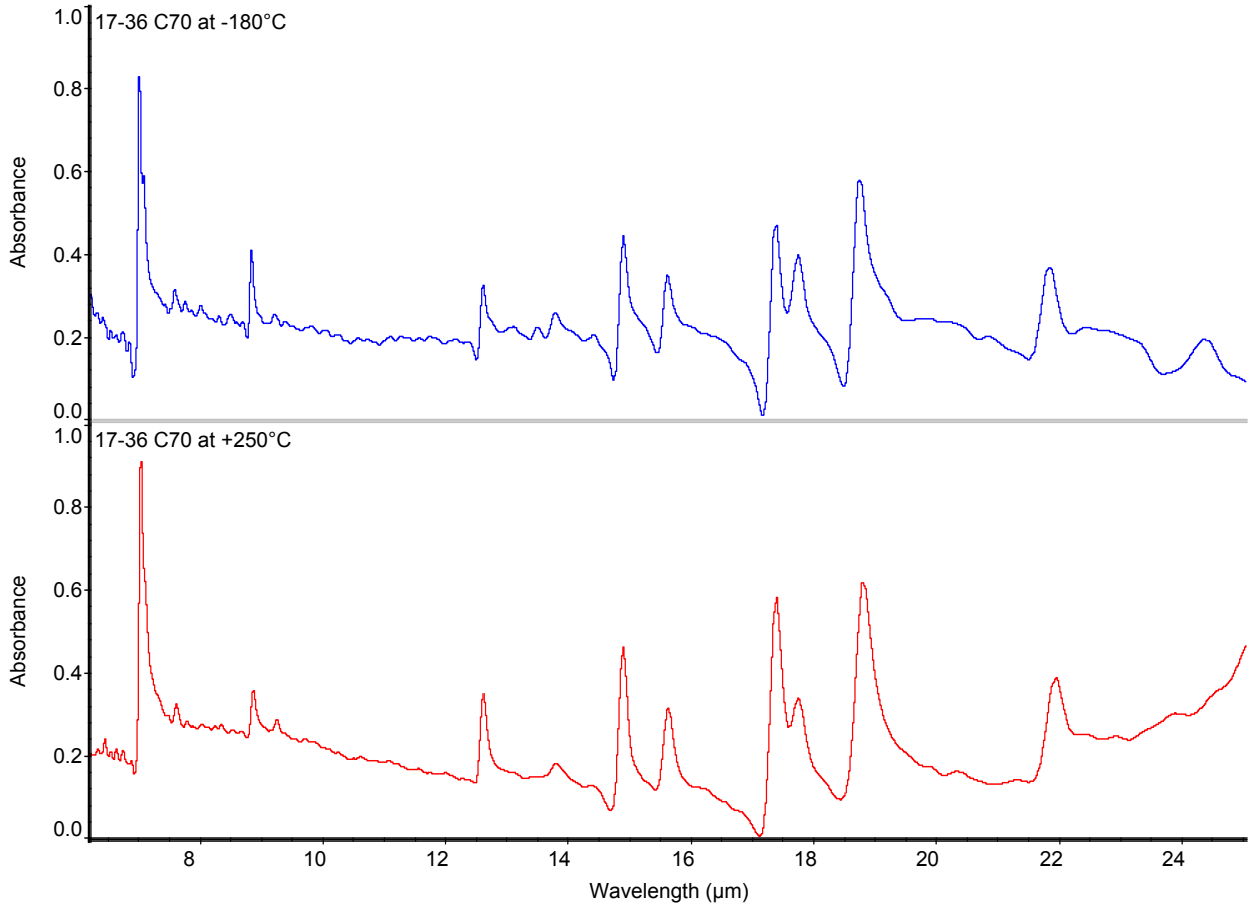

Fig. 5 – FT-IR spectra of C_{70} in KBr matrix recored at -180°C (spectrum at the top of the figure) and at +250°C (spectrum at the bottom of the figure) in the range between 6.0 and 26.0 µm.

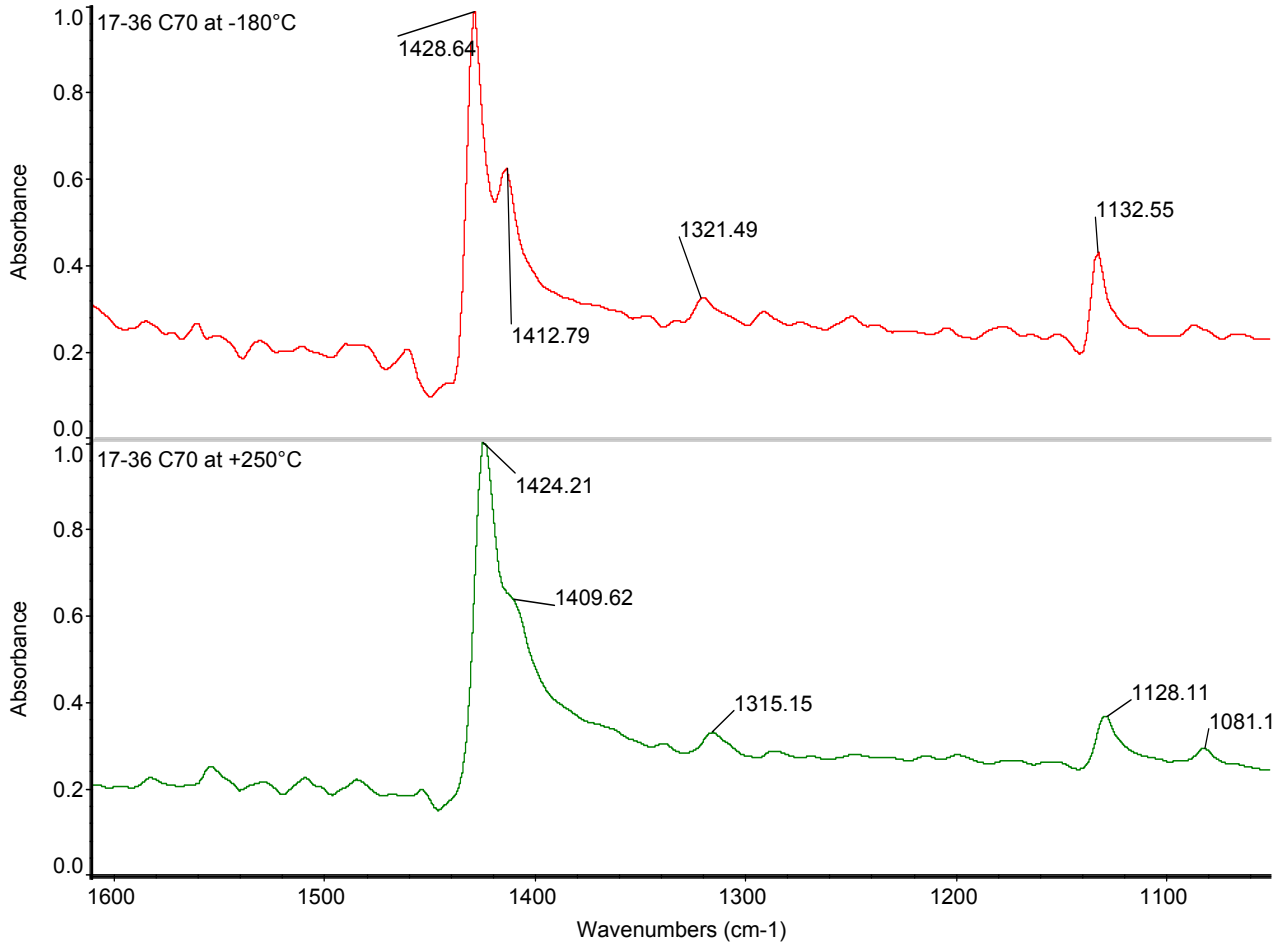

Fig. 6 – FT-IR spectra of C_{70} in KBr matrix recored at -180°C (spectrum at the top of the figure) and at +250°C (spectrum at the bottom of the figure) in the range between 1600 and 1000 cm^{-1}.

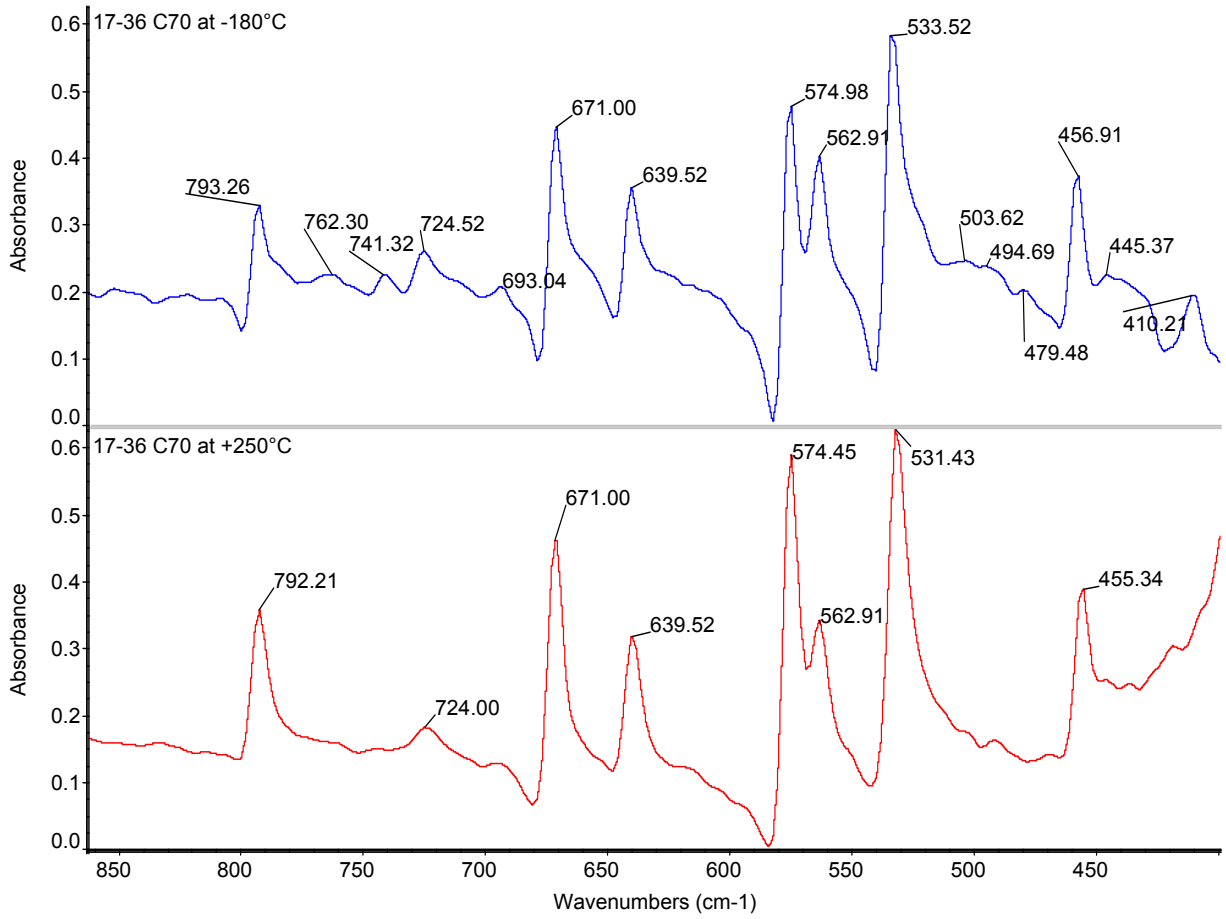

Fig. 7 – FT-IR spectra of C_{70} in KBr matrix recored at -180°C (spectrum at the top of the figure) and at +250°C (spectrum at the bottom of the figure) in the range between 900 and 400 cm^{-1}.

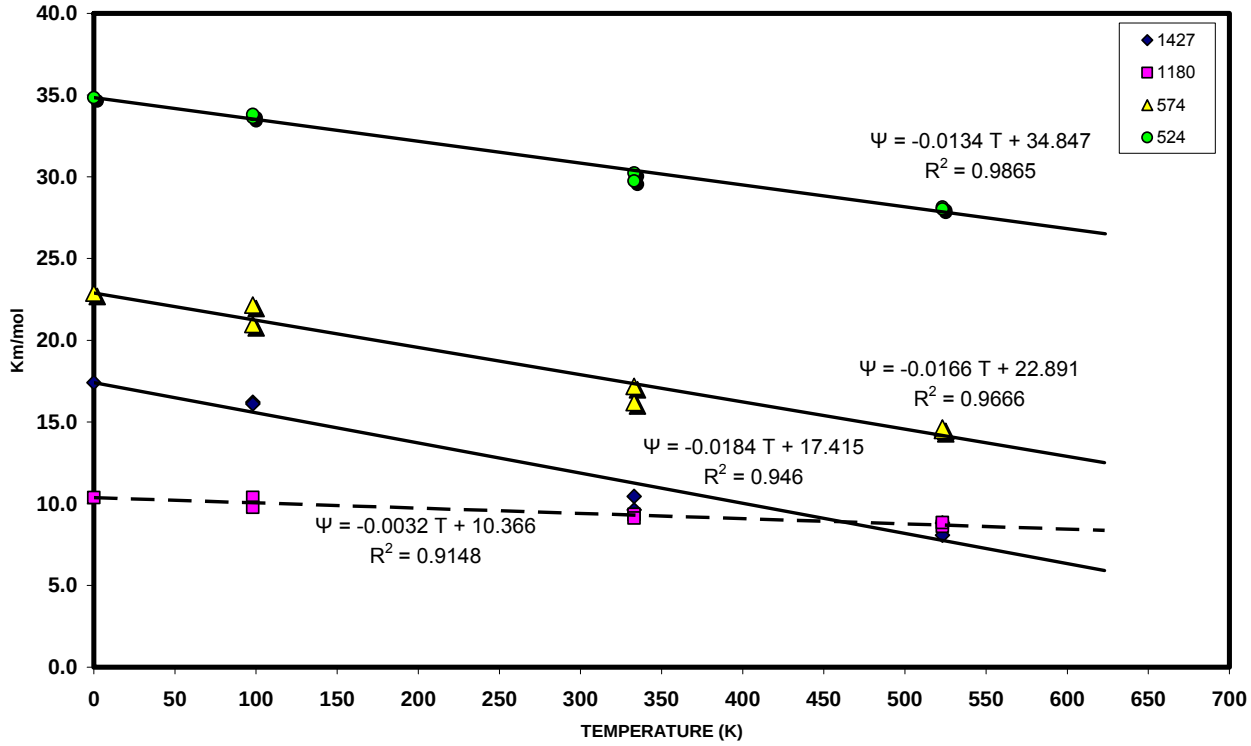

Fig. 8 – Dependence of integrated absorptivity Ψ (Km/mol) from absolute temperature (Kelvin) of the four infrared absorption bands of C_{60} fullerene.

TABLE 6 - INTEGRATED MOLAR ABSORPTIVITIES OF C_{60} AT DIFFERENT TEMPERATURES

Kelvin ------>	0	98	98	333	333	523	523
cm^{-1}	Km/mol	Km/mol	Km/mol	Km/mol	Km/mol	Km/mol	Km/mol
1427	17.4	16.2	16.1	10.4	9.6	8.8	8.1
1180	10.4	10.4	9.8	9.4	9.1	8.6	8.8
574	22.9	22.2	21.0	16.2	17.2	14.5	14.6
524	34.8	33.6	33.8	30.2	29.7	28.1	28.0

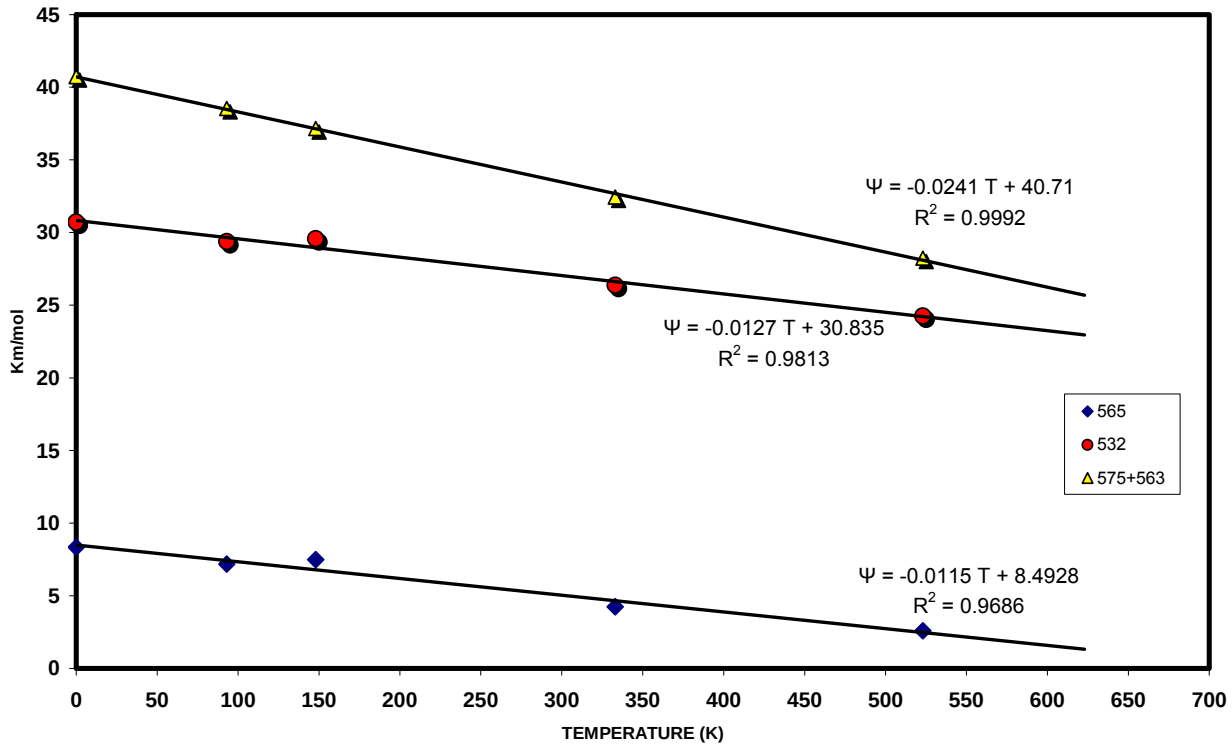

Fig. 9 – Dependence of integrated absorptivity Ψ (Km/mol) from absolute temperature (Kelvin) of a series of selected infrared absorption bands of C_{70} fullerene.

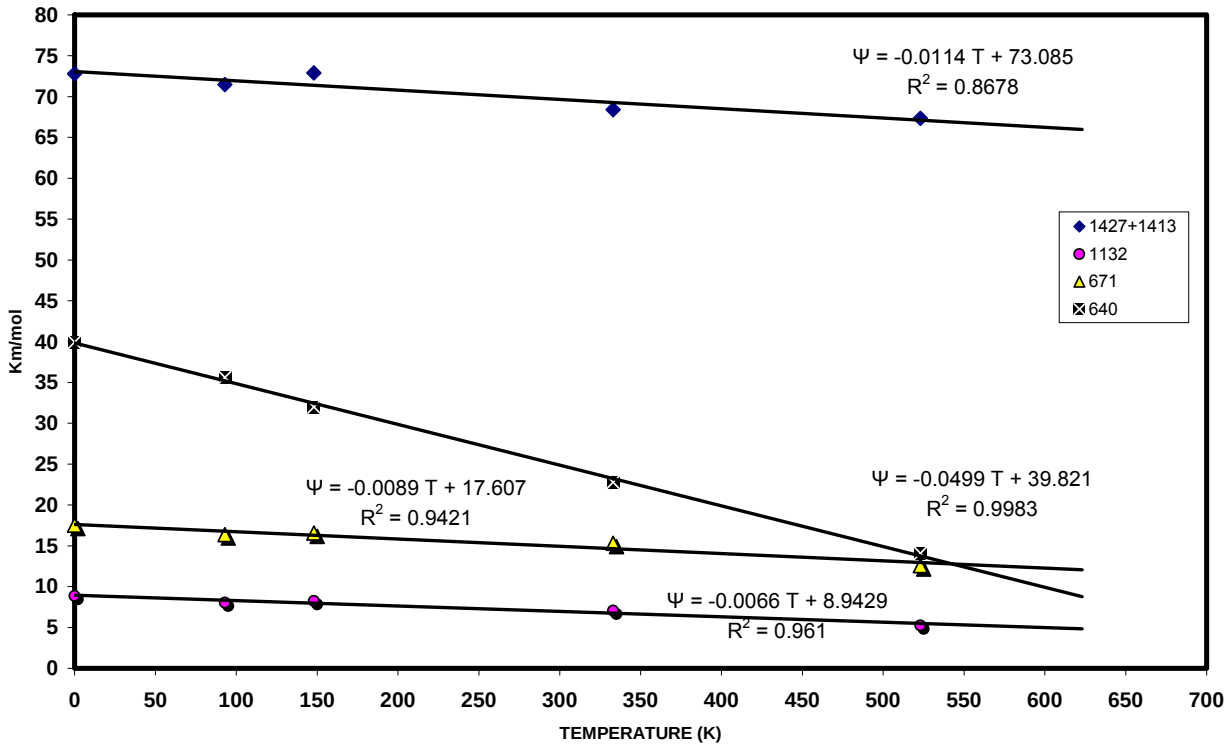

Fig. 10 – Dependence of integrated absorptivity Ψ (Km/mol) from absolute temperature (Kelvin) of another series of selected infrared absorption bands of C_{70} fullerene.

TABLE 7 - INTEGRATED MOLAR ABSORPTIVITIES OF C_{70} AT DIFFERENT TEMPERATURES

Kelvin ------>	0	93	148	333	523
cm^{-1}	Km/mol	Km/mol	Km/mol	Km/mol	Km/mol
1427+1413	72.8	71.5	72.9	68.4	67.3
1427	16.2	18.2	17.8	22.5	
1413	3.3	3.2	1.8	2.2	
1132	8.9	8.0	8.2	7.0	5.3
792	7.3	7.5	6.4	7.6	7.2
723	2.1	2.1	1.7	1.5	1.5
671	17.5	16.4	16.6	15.3	12.6
640	39.9	35.6	32.0	22.8	14.1
574	7.2	7.1	7.3	10.6	8.2
565	8.3	7.2	7.5	4.2	2.6
532	30.7	29.4	29.6	26.4	24.3
455	6.6	6.3	7.0	5.8	5.8
575+563	40.7	38.5	37.2	32.4	28.2